

Article

Evolution of quasiperiodic structures in non-ideal hydrodynamic description of phase transitions

D. N. Voskresensky ^{1,2}¹ Joint Institute for Nuclear Research, RU-141980 Dubna, Moscow region, Russia² National Research Nuclear University (MEPhI), Kashirskoe shosse 31, 115409 Moscow, Russia

* Correspondence: d.voskresen@gmail.com

Academic Editor: name

Version January 30, 2020 submitted to Universe

Abstract: Various phase transitions could have taken place in the early Universe, and may occur in the course of heavy-ion collisions and supernova explosions, in proto-neutron stars, cold compact stars, and in the condensed matter at terrestrial conditions. Most generally, the dynamics of the density and temperature at first- and second-order phase transitions can be described with the help of the equations of non-ideal hydrodynamics. In the given work some novel solutions are found describing the evolution of quasiperiodic structures that are formed in the course of the phase transitions. Although this consideration is very general, particular examples of quark-hadron and nuclear liquid-gas first-order phase transitions to the uniform $k_0 = 0$ state and pion condensate second-order phase transition to non-uniform $k_0 \neq 0$ state in dense baryon matter are considered.

Keywords: dynamics of phase transitions; spinodal instability; heavy-ion collisions; neutron stars

1. Introduction

Cosmological observations of the two last decades [1] supplied us with some extraordinary results and puzzles, in particular with the fact that the Universe undergoes an accelerated expansion and that only 5% of its mass is in baryons, 26% is in a dark matter and remaining part is in a dark energy. It is commonly believed that at least two cosmic phase transitions have occurred in the early Universe, the electro-weak and the QCD phase transitions [2,3]. The Standard Model of particle physics predicts that after the inflation the hot expanding Universe was filled with deconfined quarks, in the state of quark-gluon plasma [4]. This view on the early Universe is supported by simulations done in various cosmological and relativistic heavy ion collision models [5,6] and by the lattice calculations [7]. The quark-gluon plasma in baryon-poor matter persists down to a temperature $T \simeq 160$ MeV. However the Standard Model does not account for the presence of the dark matter, with which additional cosmic phase transitions may be associated during cooling of the expanding Universe to its present temperature $T \simeq 2.7$ K.

Another piece of important information about strongly interacting matter can be extracted from neutrino and photon radiation of compact stars formed in supernova events [8,9] and from analysis of gravitational waves in gamma ray bursts. A strong phase transition may result in a second neutrino burst if it occurred during supernova explosion and a hot neutron star formation or right after [9,10]. It might be associated with a significant delay of the heat transport to the neutron-star surface, if the system is close to the pion-condensate phase transition. Recently new arguments have been expressed for that indeed two neutrino bursts were measured during 1987A explosion, one delayed respectively other by 4.7h, cf. [11]. The second burst and a blowing of some amount of matter could be then related to the phase transition of the neutron star to the pion condensate state. In old neutron stars the first-order phase transition, if occurred, could result in a strong star-quake [9,12]. Detection of merging

compact stars in the gravitational wave spectra [13] and detection of massive compact stars [14–17] provide constraints on the equation of state of strongly interacting dense matter and strong phase transitions in it.

Experimental study of the ultrarelativistic heavy-ion collisions helps to simulate at the terrestrial conditions the processes have occurred in the very early Universe, in supernova explosions and in gamma ray bursts. Experimental data and lattice calculations [7] indicate that the hadron-quark transition in heavy-ion collisions at RHIC and LHC collision energies is the crossover transition, cf. [18–20]. For lower collision energies relevant for NICA and FAIR facilities one expects to find signatures of the strong first-order quark-hadron phase transition [21]. There are experimental evidences that in the very low-energetic heavy-ion collisions of approximately isospin-symmetrical nuclei there occurs the first-order nuclear liquid-gas phase transition (for temperatures $T \lesssim 20$ MeV and baryon densities $n \lesssim 0.7n_0$, where n_0 is the nuclear saturation density) [22–24].

In a many-component system a mechanical instability is accompanied by a chemical instability, see Ref. [25,26]. The inclusion of the Coulomb interaction, see Refs. [27,28], leads to a possibility of the pasta phase in the neutron star crusts for densities $0.3n_0 \lesssim n \lesssim 0.7n_0$. For higher densities in dense neutron star interiors there may appear phase transitions to the pion [9,29], kaon [30,31], charged rho [32] condensate states and to the quark matter [30,33–36]. The quark-hadron, pion, kaon and charged rho-meson condensate phase transitions may occur during iso-entropical falling of the baryon-rich matter in the supernova explosions [8], in proto-neutron stars and in cold compact stars, cf. [9]. In some models these phase transitions are considered as first order phase transitions leading to mixed phases in dense matter. Formation of the pasta non-uniform phases is one of the possibilities [31,35,36]. Add here possibilities of the phase transitions between various superfluid [37,38] and ferromagnetic-superfluid [39] phases in the cold neutron stars and in the color-superconducting hybrid compact stars [40], as well as numerous possibilities of the phase transitions in the condensed matter physics at terrestrial conditions, like liquid-gas, liquid-glass, glass-metal transitions, etc.

The liquid-gas phase transition, transition to the superfluid state in quantum liquids and many other transitions occur to the uniform state characterized by the wave number $k_0 = 0$. Other phase transitions, like the transitions in solids and liquid crystals, are the transitions to the inhomogeneous states characterized by the non-zero wave-vectors, $\vec{k}_{0,i} \neq 0$, cf. [41,42]. In glasses the order, characterized by $k_0 \neq 0$ appears at rather short distances but disappears at long distances [42]. The phase transition to the pion condensate state [9,29] possible in interiors of neutron stars may occur due to a strong p -wave pion-baryon attraction, which increases with increase of the baryon density. Thereby the pion condensation occurs in non-uniform state, $k_0 \neq 0$. Perhaps the antikaon condensation in dense baryon matter also occurs to the non-uniform state, $k_0 \neq 0$, cf. [43].

Some of the mentioned phase transitions, as the transition of the normal matter to superfluid in metals and in ^4He , are transitions of the second order [44]. Other mentioned above phase transitions, such as the liquid-gas phase transition, are transitions of the first order. Search for the critical endpoint separating the crossover and first-order quark-hadron transitions is one of the benchmarks for the future experiments at NICA and FAIR.

In early Universe, at the processes of the formation of compact stars in supernova explosions, collisions of compact binary stars, and in heavy-ion collisions one deals with a rapid thermalization of a strongly interacting quark-gluon matter and then the hadronic matter. These processes can be described within non-ideal hydrodynamics, where viscosity and thermal conductivity effects are of crucial importance. The dynamics of the phase transitions also can be considered within non-ideal hydrodynamics, cf. [42,45–47].

Below some novel solutions will be found describing evolution of periodic structures at the second-order phase transitions to the non-uniform state with the wave number $k_0 \neq 0$, and quasiperiodic time-dependent structures appearing in the course of the spinodal instabilities at the first order phase transitions to the uniform state with $k_0 = 0$ and in the dynamics of the second-order phase transitions occurring in the uniform state. Although consideration is very general, as specific

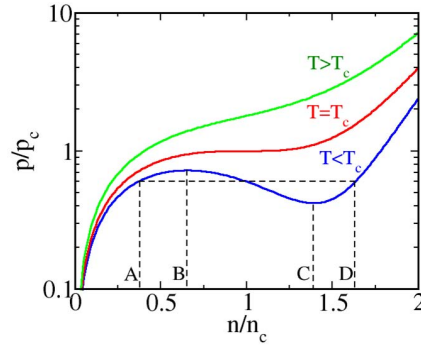


Figure 1. Schematic pressure isotherms as functions of the number density n at a liquid-gas-like phase transition. P_c , n_c and T_c are the pressure, density and temperature at the critical point.

examples, quark-hadron and nuclear liquid-gas first-order phase transitions and the pion condensation second-order transition will be considered.

The presentation is organized as follows. In Sect. 2 main features of the van der Waals-like equation of state are reminded. In Sect. 3 hydrodynamical description is formulated for the description of the first- and second-order phase transitions to the uniform $k_0 = 0$ state and for the second-order phase transition to the nonuniform, $k_0 \neq 0$, state in assumption of a small overcriticality. Dynamics of seeds at the first-order phase transition from a metastable to the stable state is considered in Sect. 4. Dynamics of fluctuations in unstable region is studied in 5. Some novel solutions describing time evolution of quasiperiodic and periodic structures are found. Sect. 6 contains some concluding remarks.

2. van der Waals-like equation of state for description of first-order phase transitions

The dynamical trajectories of the expanding baryon-rich matter in the heavy-ion collisions and of the falling matter in supernova explosions till a phase transition did not occur can be characterized by approximately conserved entropy, whereas the volume V and the temperature T are changed with the time. In the simplest case of one-component matter, e.g. the baryon matter, the pressure – baryon number density isotherms $P(n)|_T$ describing the liquid-like (with a higher density) or gas-like (with a smaller density) states demonstrate a monotonous behavior for the values of the temperature T above the critical temperature of the first-order liquid-gas type phase transition. However $P(n)|_T$ isotherms acquire a convex-concave form for T below the critical temperature [42], see Fig. 1. The horizontal dashed line connecting points A and D shows the Maxwell construction (MC) describing thermal equilibrium of phases. At equilibrium the baryon chemical potentials are $\mu_A = \mu_D$. The interval AB corresponds to a metastable supercooled vapor (SV) and the interval CD relates to a metastable overheated liquid (OL). The interval BC shows unstable spinodal region.

Adiabatic trajectories, short dashed lines s_{cr} and s_m , where $\tilde{s} \equiv s/n \simeq \text{const}$, s is the entropy density, are shown in Fig. 2 on the plot of $T/T_{cr} = f(n/n_{cr})$. The upper convex curve (MC, bold solid line) demonstrates the boundary of the MC, the bold dashed line, ITS, shows the boundary of the isothermal spinodal region and the bold dash-dotted curve AS, indicates the boundary of the adiabatic spinodal region. At the ITS line $u_T^2 = (\partial P / \partial \rho)_T = 0$ and at AS line, $u_{\tilde{s}}^2 = (\partial P / \partial \rho)_{\tilde{s}} = 0$, where u_T and $u_{\tilde{s}}$ have the meaning of the isothermal and adiabatic sound velocities, respectively, $\rho = m^*n$, m^* is the baryon quasiparticle mass. The supercooled vapor (SV) and the overheated liquid (OL) regions are situated between the MC and the ITS curves, on the left and on the right, respectively. For $\tilde{s}_{cr} > \tilde{s} > \tilde{s}_{MC2}$, where \tilde{s}_{cr} is the value of the specific entropy \tilde{s} at the critical point and the line with \tilde{s}_{MC2} in the example shown in Fig. 2 passes through the point $n/n_{cr} = 3$ at $T = 0$, the system traverses the OL state (the region OL in Fig. 2), the ITS region (below the ITS line) and the AS region (below the AS line). For $\tilde{s} > \tilde{s}_{cr}$ the system trajectory passes through the SV state (the region SV in Fig. 2) and the

ITS region. Note that in reality for the quark-hadron first-order phase transition the phase diagram

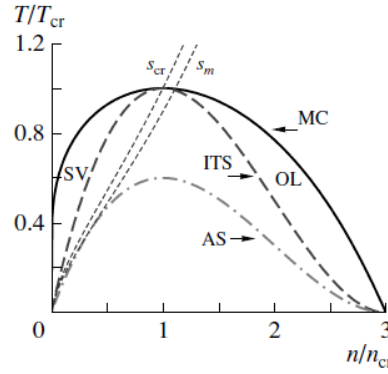


Figure 2. The phase diagram of the van der Waals equation of state on $T(n)$ -plane. The bold solid, dashed and dash-dotted curves show boundaries of the MC, the spinodal region at $T = \text{const}$ and $\bar{s} = \text{const}$, respectively. The short dashed lines show two adiabatic trajectories of the system evolution: the curve labeled s_{cr} passes through the critical point; s_m , through the maximum pressure point $P(n_{P,max})$ on the $P(n)$ plane. Figure is adopted from [47].

looks a bit different, since then T_{cr} increases with a decrease of the baryon density [48,49]. However this peculiarity does not change a general analysis given here.

After the system enters the region of the first-order phase transition of the liquid-gas type the approximation of constant entropy fails and the description of the dynamics of the system needs solution of non-ideal hydrodynamical equations [45–47]. Similarly, the description of the dynamics of the second-order phase transition needs solution of non-ideal hydrodynamical equations in the case, when the density and the temperature (or entropy) can be considered as appropriate order parameters.

3. Hydrodynamical description of first- and second-order phase transitions at small overcriticality

Further assume that the dynamics of a second order phase transition and of a first-order phase transition can be described by the variables n and s (or T), cf. [45–47]. Also, assume that the system is rather close to the critical point of the phase transition. Since all the processes in the vicinity of the critical point are slowed down, the velocity of a seed of a new phase prepared in the old phase, \vec{u} , is much less than the mean thermal velocity and one may use equations of non-relativistic non-ideal hydrodynamics: the Navier-Stokes equation, the continuity equation, and equation for the heat transport, even if one deals with violent heavy-ion collisions:

$$m^* n [\partial_t u_i + (\vec{u} \nabla) u_i] = -\nabla_i P + \nabla_k \left[\eta \left(\nabla_k u_i + \nabla_i u_k - \frac{2}{\nu} \delta_{ik} \text{div} \vec{u} \right) + \zeta \delta_{ik} \text{div} \vec{u} \right], \quad (1)$$

$$\partial_t n + \text{div}(n \vec{u}) = 0, \quad (2)$$

$$T \left[\frac{\partial s}{\partial t} + \text{div}(s \vec{u}) \right] = \text{div}(\kappa \nabla T) + \eta \left(\nabla_k u_i + \nabla_i u_k - \frac{2}{\nu} \delta_{ik} \text{div} \vec{u} \right)^2 + \zeta (\text{div} \vec{u})^2. \quad (3)$$

Here, as above, n is the number density of the conserving charge, to be specific, the baryon density, m^* is the baryon quasiparticle mass, P is the pressure. The quantities η and ζ are the shear and bulk viscosities, ν shows the geometry of the seed under consideration (droplets, rods, slabs), κ is the thermal conductivity.

All thermodynamical quantities can be expanded near a reference point (n_r, T_r) , which we assume to be close to the critical point but still outside the fluctuation region, which we assume to be narrow. This circumstance is important for the determination of the specific heat density $c_{V,r}$ and, m.b.,

transport coefficients, which may diverge in the critical point, whereas other quantities are smooth functions of n, T and calculating them one can put $n_r = n_{cr}, T_r = T_{cr}$.

The Landau free energy counted from the value at $n_r \simeq n_{cr}, T_r \simeq T_{cr}$ in the variables $\delta n = n - n_{cr}, \delta T = T - T_{cr}, \delta(\delta F_L)/\delta(\delta n) = P - P_f + P_{MC}$ can be presented as [45–47]

$$\delta F_L = \int \frac{d^3x}{n_{cr}} \left\{ \frac{cm^*[\nabla(\delta n)]^2}{2} + \frac{\lambda m^{*3}(\delta n)^4}{4} - \frac{\lambda v^2 m^*(\delta n)^2}{2} - \epsilon \delta n \right\} + \delta F_L(k_0), \quad (4)$$

where $\epsilon = P_f - P_{MC} \simeq n_{cr}(\mu_i - \mu_f)$ is expressed through the (final) value of the pressure after the first-order phase transition has occurred and the pressure at the MC, μ_i and μ_f are the chemical potentials of the initial and final configurations (at fixed P and T). The quantity $\epsilon \neq 0$, if one deals with a first-order phase transition, and $\epsilon = 0$, if a transition is of the second order. The maximum of the quantity ϵ is $\epsilon_m = 4\lambda v^3/(3\sqrt{3})$. For the description of phase transitions to the uniform state, $k = 0$, one may retain only the term $\propto c[\nabla(\delta n)]^2$ in the expansion of the free energy in the density gradients using $c > 0$. For the description of phase transitions to the non-uniform state, $k_0 \neq 0$, one should perform expansion retaining at least terms up to $\propto d[\Delta(\delta n)]^2$ assuming $c < 0$ and $d > 0$. Therefore the last term in (4) appears only, if $k = k_0 \neq 0$ [42], like for the phase transition to the solid state, liquid crystal state, or a pion condensate state in a dense nuclear matter. Then for $k_0 \neq 0$ and $c < 0, d > 0$ we have

$$\delta F_L(k_0) = \int \frac{d^3x}{n_{cr}} \left\{ \frac{dm^*}{2} (\Delta \delta n)^2 + \left(\frac{cm^*k_0^2}{2} - \frac{dm^*k_0^4}{2m^*} \right) (\delta n)^2 \right\}, \quad (5)$$

where $k_0^2 = -\frac{c}{2d} > 0$ follows from minimization of $\delta F_L(k_0)$. In case of the phase transition to the uniform state one should put $k_0 = 0, d = 0$ (then $\delta F_L(k_0) = 0$) and $c > 0$. Then the first term $\propto c$ in Eq. (4) is associated with the positive surface tension, $\delta F_L^{\text{surf}} = \sigma S$, where S is the surface of the seed.

The Landau free energy density and pressure as functions of the order parameter $\delta\rho$ for the equation of state determined by Eq. (4) are shown in Fig. 3. For $\epsilon = 0$ two minima of the Landau free energy coincide and correspond to the MC on the curve $\delta P(1/\rho)$ (shown by horizontal lines in the plot $\delta P(\delta\rho)$ in the right panel). If in the initial state $(\delta\rho)_i = \rho_i - \rho_{cr} = 0$, we deal with the spontaneous symmetry breaking and the second-order phase transition. For $(\delta\rho)_i = \rho_i - \rho_{cr} \neq 0, \epsilon > 0$ or $\epsilon < 0$, we may deal either with the first-order phase transition from the metastable to the stable state, if ρ_i corresponds to the metastable state, or with the second order phase transition either to the metastable state or to the stable state, otherwise. For $\epsilon > 0$ (solid lines) the liquid state is stable and the gas state is metastable (SV), and for $\epsilon < 0$ (dash-dotted lines) the liquid state is metastable (OL), whereas the gas state is stable. The dynamics of the transition starting from a point within spinodal region for $\epsilon \neq 0$ (but small) is described similarly to that for the second-order phase transition for $\epsilon = 0$.

For the purely van der Waals equation of state (in this case $k_0 = 0$) one gets [46]:

$$v^2(T) = -4 \frac{\delta T n_{cr}^2 m^{*2}}{T_{cr}}, \quad \sigma = \sigma_0 \frac{|\delta T|^{3/2}}{T_{cr}^{3/2}}, \quad \sigma_0^2 = 32m^* n_{cr}^2 T_{cr} c. \quad (6)$$

Applying operator div to Eq. (1) and replacing $\text{div} \vec{u}$ from Eq. (2) for small $\delta\rho$ and u , keeping only linear terms in u , that is legitimate, since near the critical point processes develop slowly ($v^2 \propto -\delta T$), we rewrite Eq. (1) as

$$-\frac{\partial^2 \delta n}{\partial t^2} = \Delta \left[c\Delta \delta n + \lambda v^2 \delta n - \lambda m^{*2} (\delta n)^3 + \epsilon/m^* - (m^* n_{cr})^{-1} (\tilde{\nu} \eta_{cr} + \zeta_{cr}) \frac{\partial \delta n}{\partial t} \right] - \Delta \left[d\Delta^2 \delta n + (ck_0^2 + dk_0^4) \delta n \right], \quad (7)$$

$\tilde{\nu} = 2(\nu - 1)/\nu$, cf. [9,42,46]. Second line in Eq. (7) yields non-zero term only for the description of the condensation to the inhomogeneous state.

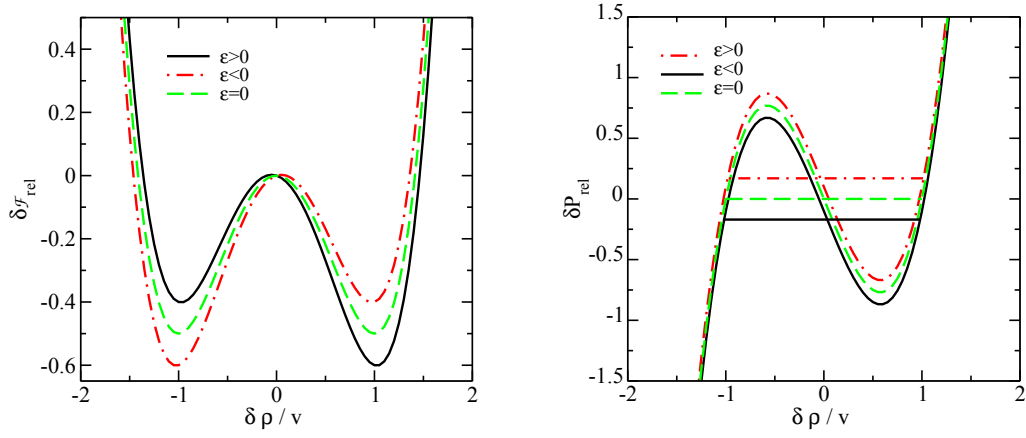


Figure 3. The Landau free energy density $\delta \mathcal{F}_{\text{rel}} = \delta \mathcal{F}_L / \mathcal{F}_L(T_{cr}, \rho_{cr})$ and the value $\delta P_{\text{rel}} = \rho_{cr} \frac{\delta [\mathcal{F}_L(T, \delta \rho)]}{\delta (\delta \rho)} \Big|_T / P(T_{cr}, \rho_{cr})$, as functions of the order parameter $\delta \rho = m^* \delta n$ for the EoS determined by Eq. (4), at $T < T_{cr}$. Dash horizontal line ($\epsilon = 0$) in the right panel shows MC. Figure is adopted from [46].

Consider $T < T_{cr}$. In the dimensionless variables $m^* \delta n = v\psi$, $\tau = t/t_0$, $\xi_i = x_i/l$, $i = 1, \dots, \nu$, $\nu = 3$ for seeds of spherical geometry, Eq. (7) is presented as

$$-\beta \frac{\partial^2 \psi}{\partial \tau^2} = \Delta_{\xi} \left(\Delta_{\xi} \psi + 2\psi(1 - \psi^2) + \tilde{\epsilon} - \frac{\partial \psi}{\partial \tau} - \frac{\lambda v^2 d}{2c^2} \Delta_{\xi}^2 \psi + \frac{2(ck_0^2 + dk_0^4)}{\lambda v^2} \psi \right), \quad (8)$$

$$l = \left(\frac{2c}{\lambda v^2} \right)^{1/2}, \quad t_0 = \frac{2\tilde{\eta}_r}{\lambda v^2}, \quad \tilde{\epsilon} = \frac{2\epsilon}{\lambda v^3}, \quad \beta = \frac{c}{\tilde{\eta}_r^2}, \quad \tilde{\eta}_r = \frac{(\tilde{v}\eta_r + \zeta_r)}{m^* n_{cr}}.$$

It is important to notice that even for $k_0 = 0$, Eq. (8) differs in the form from the standard Ginzburg-Landau equation broadly exploited in the condensed matter physics, since Eq. (8) is of the second-order in time derivatives, whereas the standard Ginzburg-Landau equation is of the first order in time derivatives. The difference disappears, if one puts the bracketed-term in the r.h.s. of Eq. (8) to zero. This procedure is however not legitimate at least for description of the order parameter on an initial time-stage, since two initial conditions, such as $\delta n(t = 0, \vec{r}) = 0$ and $\partial_t \delta n(t, \vec{r})|_{t=0} \simeq 0$, should be fulfilled to describe an initially formed fluctuation (seed). Thereby at least there exists an initial stage of the dynamics of seeds ($t \lesssim t_{\text{init}}$), which is not described by the standard Ginzburg-Landau equation [45,46]. The bracketed-term in the r.h.s. of Eq. (8) can indeed be put zero, see below, if one considers an effectively very viscous medium at $\tau \gg 1$. Also note that Eq. (8) with the bracketed-term in the r.h.s. equal zero can be derived from the first-gradient order kinetic equation of Kadanoff-Baym [50].

Eq. (8) should be supplemented by Eq. (3) for the heat transport, which owing to Eq. (2) after its linearization reads as

$$T_{cr} \left[\partial_t \delta s - s_{cr}(n_{cr})^{-1} \partial_t \delta n \right] = \kappa_r \Delta \delta T. \quad (9)$$

The variation of the temperature is related to the variation of the entropy density $s[n, T]$ by

$$\delta T \simeq T_{cr} (c_{V,r})^{-1} (\delta s - (\partial s / \partial n)_{T,cr} \delta n), \quad (10)$$

c_V is the density of the heat capacity.

3.1. Typical time scales

Let us perform some rough dimensional estimates of typical time scales in the problem. The evolution of a seed of one phase in another phase is governed by the slowest mode ($\delta\rho$ or δs , respectively). The time scale for the relaxation of the density following Eq. (8) is $t_0 \propto \tilde{\eta}$. Thus the non-zero viscosity plays the role of the driving force managing the time evolution of the density-mode. Also $t_0 \propto 1/(T_{cr} - T)$. Thereby the processes are slowed down near the critical point of the phase transition. The time scale for the relaxation of the entropy/temperature mode, following (9), is

$$t_T = R_{\text{seed}}^2 c_{V,r} / \kappa_r \propto R_{\text{seed}}^2, \quad (11)$$

i.e., relaxation time of the temperature/entropy is proportional to the surface of the seed. Thus, for $t_T(R_{\text{seed}}) < t_0$, i.e for $R_{\text{seed}} < R_{\text{fog}} = \sqrt{\kappa_r t_0 / c_{V,r}}$, where R_{fog} is the typical size of the seed at $t \sim t_0 = t_T$, dynamics of seeds is controlled by Eq. (8) for the density mode. For seeds with sizes $R_{\text{seed}} > R_{\text{fog}}$, the quantity $t_T \propto R_{\text{seed}}^2$ exceeds t_0 and growth of seeds is slowed down. Thereby, the number of seeds with the typical size $R_{\text{seed}} \sim R_{\text{fog}}$ is increased with passage of time, and a state of fog is formed. For the quark-hadron phase transition in energetic heavy-ion collisions one [46] estimates $R_{\text{fog}} \sim (0.1 - 1)$ fm and for the nuclear liquid-gas transition at low energies $R_{\text{fog}} \sim (1 - 10)$ fm $\lesssim R(t_{\text{f.o.}})$, where $R(t_{\text{f.o.}})$ is the size of the fireball at the freeze out, $t_{\text{f.o.}}$ is the fireball evolution time till freeze out.

There are only two dimensionless parameters in Eq. (8), $\tilde{\epsilon}$ and β . The parameter $\tilde{\epsilon}$ is responsible for a difference between the Landau free energies of the metastable and stable states. For $t_0 \gg t_T$ (isothermal stage), $\tilde{\epsilon} \simeq \text{const}$ and dependence on this quantity disappears because of $\Delta_{\xi} \tilde{\epsilon} \simeq 0$. Then,

dynamics is controlled by the parameter β , which characterizes an inertia. It is expressed in terms of the surface tension and the viscosity as

$$\beta = (32T_{cr})^{-1}[\tilde{\nu}\eta_r + \zeta_r]^{-2}\sigma_0^2 m^*. \quad (12)$$

The larger viscosity and the smaller surface tension, the effectively more viscous (inertial) is the fluidity of seeds. For $\beta \ll 1$ one deals with the regime of effectively viscous (inertial) fluidity and at $\beta \gg 1$ one deals with the regime of almost perfect fluidity. Estimates [46] show that for the nuclear liquid-gas phase transition typically $\beta \sim 0.01$. For the quark-hadron transition $\beta \sim 0.02 - 0.2$, even for very low value of the ratio $\eta/s \simeq 1/(4\pi)$. The latter quantity characterizes fluidity of the matter at ultra-relativistic heavy-ion collisions [20]. Thus, as we argued, in case of baryon-rich matter one deals with effectively very viscous (inertial) evolution of density fluctuations both in cases of the nuclear liquid-gas and quark-hadron phase transitions.

In neutron stars an overcritical pion-condensate drop reaches a size $R \sim 0.1$ km for $t \sim 10^{-3}$ sec. by the growth of the density mode. Then it may reach $R \sim (1 - 10)$ km for typical time t_T varying from ~ 10 sec. up to several hours (rather than for typical collapse time $\sim 10^{-3}$ sec). A delay appears owing to neutrino heat transport to the surface (effect of thermal conductivity) that strongly depends on the value of the pion softening, which is stronger for most massive neutron stars [9]. One should also take into account that the bulk viscosity is significantly increased in presence of soft modes [51,52], e.g., near the pion condensation critical point [53]. Also notice that description of the dynamics of the pion-condensate phase transition is specific, since the transition occurs to the inhomogeneous liquid-crystal-like state characterized by $\vec{k} \neq 0$. Seeds of the liquid-crystal-like state prove to be elongated in the process of their growth [42], similar effect is observed in liquid crystals.

Thus, interplay between viscosity, surface tension, and thermal conductivity effects is responsible for the typical time and size scales of fluctuations.

3.2. Stationary solutions

Now let us find stationary solutions of Eq. (7). For the condensation in the state $k \neq 0$ we find solution in the form

$$m^* \delta n = a[\sin(kx + \chi) + \frac{c_1 \tilde{\omega}^2(k^2)}{\tilde{\omega}^2(9k^2)} \sin(3kx + \chi) + \dots] + O(\epsilon), \quad (13)$$

where χ is a constant phase,

$$\tilde{\omega}^2(k^2) = -\lambda v^2 + ck^2 + dk^4 - ck_0^2 - dk_0^4. \quad (14)$$

For the condensation in the uniform state $k_0 \neq 0$, $c < 0$, $d > 0$ the gap $\tilde{\omega}^2(k^2)$ has a minimum for $k = k_0$. The phase transition arises for $\tilde{\omega}^2(k_0^2) < 0$. Setting (13) in Eq. (7) we find

$$a^2 = -\frac{4}{3} \tilde{\omega}^2(k_0^2) / \lambda > 0, \quad c_1 = -1/3. \quad (15)$$

Minimization of the free energy in k yields $k = k_0$ and $\tilde{\omega}^2(k_0^2) = -\lambda v^2$, $\tilde{\omega}^2(k_0^2) > 0$ for $T > T_{cr}$ and $\tilde{\omega}^2(k_0^2) < 0$ for $T < T_{cr}$, $\tilde{\omega}^2(9k_0^2) = -\lambda v^2 + 16c^2/d \gg |\tilde{\omega}^2(k_0^2)|$. Thereby with appropriate accuracy we may use $\delta n \simeq a[\sin(k_0 x + \chi)]$ that yields $\delta F_L(k_0) \simeq -\lambda v^4 V / (6m^* n) + O(\epsilon^2)$, where V is the volume of the system. Thus solution (13) describes the stationary state at the second-order phase transition.

For the condensation in the uniform state $k_0 = 0$ we have [46]

$$\tilde{\omega}^2(k^2) = -\lambda v^2 + ck^2, \quad k^2 < \lambda v^2 / c, \quad c > 0. \quad (16)$$

Two spatially constant stationary solutions minimizing the free energy for $T < T_{cr}$ correspond to $k = 0$. They describe metastable and stable states:

$$\delta n_{st} \simeq \pm v/m^* + \epsilon/(2\lambda v^2 m^*). \quad (17)$$

The free energy corresponding to these solutions is given by

$$\delta F_L(k = 0, k_0 = 0) \simeq -\frac{\lambda v^4 V}{4m^* n_{cr}} \left(1 \pm \frac{4\epsilon}{\lambda v^3}\right). \quad (18)$$

For $k \neq 0$ solutions in the form (13) are valid for $|\tilde{\omega}^2(k^2)| \ll \tilde{\omega}^2(9k^2)$ and they yield for $k_0 = 0$:

$$\delta F_L(k \neq 0, k_0 = 0) \simeq -\frac{\lambda v^4 (1 - ck^2/(\lambda v^2)) V}{6m^* n_{cr}}. \quad (19)$$

Although the minimum of the free energy for $k_0 = 0$ is given by (18) corresponding to solutions (17) obtained for $k = 0$, rather than by solutions of (13) corresponding to the free energy (19), nevertheless, as we will demonstrate below, solutions (13) characterising by $k \neq 0$ have a physical meaning.

4. Dynamics of seeds at first-order phase transition from metastable state to stable state

Consider the limit of a high thermal conductivity, when in Eq. (7) the temperature can be put constant. Solution of Eq. (7) describing dynamics of the density fluctuation developing from the metastable state to the stable state is then presented in the form [47]

$$\delta n(t, r) \simeq \frac{v(T)}{m} \left[\pm \text{th} \frac{r - R_{\text{seed}}(t)}{l} + \frac{\epsilon}{2\lambda v^3(T)} \right] + (\delta n)_{\text{cor}}, \quad (20)$$

where the upper sign corresponds to the evolution of bubbles of the gas and the lower-sign solution describes evolution of droplets of liquid for $\nu = 3$, and the solution is valid for $|\epsilon/(\lambda v^3(T))| \ll 1$. Compensating correction $(\delta n)_{\text{cor}}$ is introduced to fulfill the baryon number conservation. Considering spatial coordinate r in the vicinity of a bubble/droplet boundary we get equation describing evolution of the seed size [46,47]:

$$\frac{m^{*2} \beta t_0^2}{2l} \frac{d^2 R_{\text{seed}}}{dt^2} = m^{*2} \left[\frac{3\epsilon}{2\lambda v^3(T)} - \frac{2l}{R_{\text{seed}}} \right] - \frac{m^{*2} t_0}{l} \frac{dR_{\text{seed}}}{dt}. \quad (21)$$

This equation reminds the Newton second law for a one-dimensional system, where the quantity $M = \frac{m^{*2} \beta t_0^2}{2l} \propto (T_{cr} - T)^{-3/2}$ has a meaning of a mass, $m^{*2} \left[\frac{3\epsilon}{2\lambda v^3(T)} - \frac{2l}{R_{\text{seed}}} \right]$ is an external force and $-\frac{m^{*2} t_0}{l} \frac{dR_{\text{seed}}}{dt}$ is the friction force, with a viscous-friction coefficient proportional to an effective viscosity and inversely proportional to $\sqrt{T_{cr} - T}$. Following Eq. (21) a bubble of an overcritical size $R_{\text{seed}} > R_{cr} = 4l\lambda v^3(T)/(3\epsilon)$ of the stable gas phase, or respectively a droplet of the stable liquid phase, been initially prepared in a fluctuation inside a metastable phase, then grow. On an early stage of the evolution the size of the overcritical bubble/droplet $R_{\text{seed}}(t)$ (for $R_{\text{seed}} > R_{cr}$) grows with an acceleration. Then it reaches a steady growth regime with a constant velocity $u_{\text{as}} = \frac{3\epsilon l}{\lambda v^3(T) t_0} \propto |(T_{cr} - T)/T_{cr}|^{1/2}$. In the interior of the seed $\delta n \simeq \mp v(T)/m^*$. The correction $(\delta n)_{\text{cor}} \simeq v(T) R_{\text{seed}}^3(t)/(m^* R^3)$ is very small for $R_{\text{seed}}(t) \ll R$, where R is the radius of the whole system. In cases of the quark-hadron and nuclear liquid-gas phase transitions in heavy-ion collisions $R(t)$ is the radius of the expanding fireball. Usage of the isothermal approximation in Eq. (20) needs fulfillment of inequality $t_\rho \sim \frac{R_{\text{seed}}(t_{\text{f.o.}})}{u_{\text{as}}} \gg t_T$. For $R_{\text{seed}} \sim R_{cr}$ and for $\epsilon \sim \epsilon_m$ we get $t_\rho \sim t_0$, and isothermal approximation is valid for $R_{\text{seed}} < R_{\text{fog}}$. For $\epsilon \ll \epsilon_m$ we get $t_\rho \gg t_0$ and isothermal approximation remains correct for seeds of the size $R_{\text{seed}} < R_{\text{fog}} \epsilon_m / \epsilon$.

Substituting Eq. (20) to Eq. (9) for $T \simeq \text{const}$ (that is correct in linear approximation) we obtain

$$\delta s = \left(\frac{\partial s}{\partial n} \right)_T \left\{ \frac{v(T)}{m} \left[\pm \text{th} \frac{r - R_{\text{seed}}(t)}{l} + \frac{\epsilon}{2\lambda_{cr}v^3(T)} \right] + (\delta n)_{\text{cor}} \right\}. \quad (22)$$

Note that for the description of expanding fireball formed in heavy-ion collisions the approximation of a quasi-adiabatic expansion can be used even in presence of the weak first-order phase transition (for $\delta s \ll s$ and $\delta n \ll n$). The evolution of droplets/bubbles in metastable region can be considered at fixed size of the fireball provided $t_{f.o.} \gg (t_\rho, t_T)$.

5. Dynamics of fluctuations in unstable region

5.1. Growth of fluctuations of small amplitude. Linear regime

In this section the “r”-reference point can be taken arbitrary, therefore we suppress the subscript “r”. To find solutions of the linearized hydrodynamical equations we put, cf. [47],

$$\delta n = \delta n_0 \exp[\gamma t + i\vec{k}\vec{r}] - \frac{\epsilon}{m^* \lambda v^2}, \quad \delta s = \delta s_0 \exp[\gamma t + i\vec{k}\vec{r}], \quad T = T_> + \delta T_0 \exp[\gamma t + i\vec{k}\vec{r}], \quad (23)$$

where $T_>$ is the temperature of the uniform matter. For $|\delta n| \gg |\frac{\epsilon}{m^* \lambda v^2}|$, i.e. for $\epsilon \ll \epsilon_m$, description of a fluctuation in spinodal region at the first-order phase transition and for description of the second-order phase transition are the same and we may put $\epsilon \rightarrow 0$. Then from linearized equations of non-ideal hydrodynamics (7), (9) we find the increment, $\gamma(k)$,

$$\gamma^2 = -k^2 \left[\tilde{\omega}^2(k^2) + \tilde{\eta}\gamma + \frac{u_s^2 - u_T^2}{1 + \kappa k^2 / (c_V \gamma)} \right], \quad (24)$$

where $\tilde{\eta} = \frac{(\tilde{v}\eta + \zeta)}{m^* n}$. Eq. (24) has three solutions corresponding to the growth of the density and thermal modes. For $\kappa k^2 / (c_V |\gamma|) \gg 1$ the temperature in the seed can be put constant and we may deal with only one equation for the density mode (7) that yields

$$\gamma^2 = -k^2 \left[\tilde{\omega}^2(k^2) + \tilde{\eta}\gamma \right], \quad (25)$$

from where we find two solutions for the density-modes,

$$\gamma_{1,2} = -\frac{k^2 \tilde{\eta}}{2} \pm \sqrt{\frac{k^4 \tilde{\eta}^2}{4} - k^2 \tilde{\omega}^2(k^2)}. \quad (26)$$

For $\tilde{\omega}^2(k^2) < 0$, that corresponds to the region of the phase transition, the upper-sign solution, $\gamma_1 > 0$, describes the growing mode and the lower sign solution, $\gamma_2 < 0$, describes the damping mode. For $k^2 \tilde{\eta}^2 / |\tilde{\omega}^2(k^2)| \ll 1$ we have

$$\gamma_1 \simeq \sqrt{-k^2 \tilde{\omega}^2(k^2)} - \frac{k^2 \tilde{\eta}}{2} + O(k^3 \tilde{\eta}^2 / |\tilde{\omega}(k^2)|) \quad (27)$$

for the growing mode. In the opposite limit $k^2 \tilde{\eta}^2 / |\tilde{\omega}^2(k^2)| \gg 1$ we obtain

$$\gamma_1 \simeq -\tilde{\omega}^2(k^2) / \tilde{\eta} + O(\tilde{\omega}^4(k^2) / (k^2 \tilde{\eta}^3)). \quad (28)$$

Note that in condensed matter physics a transition from a liquid to a glass state can be interpreted as a first-order phase transition occurring within a spinodal region at a very high viscosity [42]. Then there appears an order at several Å-scale, which transforms in a disorder at larger distances.

For $k_0 = 0, c > 0$, for the most rapidly growing mode (for $\gamma_m = \max\{\gamma_1\}$ corresponding to $k = k_m$) we find

$$\gamma_m \simeq \frac{\lambda v^2}{(2\sqrt{\beta} + 1)\tilde{\eta}}, \quad k_m^2 \simeq \frac{\lambda v^2 \sqrt{\beta}}{(2\sqrt{\beta} + 1)c}.$$

For $k_0 \neq 0, c < 0, d > 0$ the most rapidly growing mode corresponds to $k = k_0$, then $\tilde{\omega}^2(k_0^2) < 0$ and $|\tilde{\omega}^2(k_0^2)|$ as a function of k^2 is the largest.

5.2. Growth of fluctuations of arbitrary amplitude. Nonlinear regime

Now we will find solution of the non-linear Eq. (7). We search the solution in the form

$$m^* \delta n = af(t) \left[\sin(kx + \chi) + \frac{c_1 \tilde{\omega}^2(k^2)}{\tilde{\omega}^2(9k^2)} \sin(3kx + \chi) + \dots \right] + O(\epsilon), \quad (29)$$

as (13) with $a^2 = -\frac{4\tilde{\omega}^2}{3\lambda} > 0$ but now with $f(t)$ satisfying equation

$$\partial_t^2 f = -k^2 \tilde{\omega}^2(k^2) f(1 - f^2) - k^2 \tilde{\eta} \partial_t f. \quad (30)$$

For $k^2 \tilde{\eta}^2 / |\tilde{\omega}^2(k^2)| \gg 1$, i.e. for $\beta \ll 1$ or $\tilde{\eta} \gg \sqrt{c}$, the term $\partial_t^2 f$ in the l.h.s. of Eq. (30) can be dropped and the amplitude

$$f(t) = \frac{f_0 e^{\gamma t}}{\sqrt{1 + f_0^2 e^{2\gamma t}}}, \quad (31)$$

fulfils the resulting Eq. (30), $f_0 / \sqrt{1 + f_0^2}$ shows the amplitude of the fluctuation at $t = 0$, f_0 is an arbitrary constant. For $k \sim k_m$ at $k_0 = 0$ this solution holds for $k_m^2 \tilde{\eta}^2 / |\tilde{\omega}^2(k_m^2)| \gg 1$. For $k = k_0 \neq 0$ the criterion of applicability renders as $k_0^2 \tilde{\eta}^2 / |\tilde{\omega}^2(k_0^2)| \gg 1$. In both cases $k_0 = 0$ and $k_0 \neq 0$ with the density distribution given by (29), (31) the free energy renders

$$\delta F_L(t) = -\frac{V \tilde{\omega}^4(k^2)}{6\lambda m^* n} f^2(t) (2 - f^2(t)). \quad (32)$$

For $t \rightarrow \infty$ we have $f(t \rightarrow \infty) \rightarrow 1$ and δF_L reaches the minimum. For $k = k_0$ this value coincides with (19) given by the stationary solution.

In general case expression (31) yields an interpolation between two approximate solutions valid for the limit cases $\gamma t \ll 1$ and $\gamma t \gg 1$. Replacing (31) in Eq. (30) we obtain then the same solutions (26) as in linear case.

Let first $k_0 = 0$. For $t \rightarrow \infty$ using solution (31) at $\gamma = \gamma_m = \gamma(k_m)$ we find

$$\delta F_L(t \rightarrow \infty) = -\frac{\tilde{\omega}^4(k_m^2) V}{6\lambda m^* n}. \quad (33)$$

For the case of a large effective viscosity/inertia, $\beta \ll 1$, we obtain $\delta F_L(t \rightarrow \infty) \simeq -\frac{\lambda v^4 V}{6m^* n}$ that coincides with (19) but is still larger than the value given by (18). For the case of a small effective viscosity/inertia, $\beta \gg 1$, we find $\delta F_L(t \rightarrow \infty) \simeq -\frac{\lambda v^4 V}{24m^* n}$ that is much higher than the free energy given by both stationary solutions (18), (19). Thus one may expect that expression (33) either describes a metastable state or a state, which slowly varies on a time scale $t_k \gg t_\gamma \sim 1/\gamma_m$, reaching for $t \gg t_k$ the stationary state with the free energy given by (18). To show the latter possibility consider the case $\beta \gg 1$ and assume k

in solution (29) to be a slow function of time, i.e. $k = k(t)$, for typical time scale $t_k \gg t_\gamma$. One can see that for $R_{\text{seed}} \ll t_k |u_T|$ the quantity $k(t)$ satisfies equation $(d^2k/dt^2) = -k^2 \tilde{\eta} (dk/dt)$ with the solution

$$k(t) = k_{00} [1 + \tilde{\eta} \lambda v^2 t / (3c)]^{-1/2} \quad (34)$$

such as $k(t \rightarrow \infty) \rightarrow 0$ and the free energy for $t \rightarrow \infty$ indeed reaches the limit (18) provided we set $\sin \chi \simeq \frac{\sqrt{3}}{2} - \frac{\sqrt{3} m^* \tilde{\epsilon}}{8}$. From Eq. (34) we easily find that the typical time scale is $t_k \sim \beta t_0$ and we check that indeed $t_k \gg t_\gamma$. For $R_{\text{seed}} \gtrsim t_k |u_T| \sim l \sqrt{\beta}$ the solution (29) with (34) does not hold and should be modified.

For $\beta \ll 1$, $k_0 = 0$, expression (34) with slowly varying $k(t)$ does not hold. At realistic conditions convection and sticking processes (at sizes $\sim l$) may be allowed, which destroy periodicity, and owing to these processes the system may finally reach the ground state with the free energy given by (18). Thus one possibility is that for the typical time $t \sim t_\gamma \sim t_0$ the quasiperiodic solution (33) is formed with typical $k \simeq k_m$, corresponding to a metastable state with the free energy given by (19). Such a distribution is formed most rapidly. Another possibility is that for the typical time scale $t_{\text{unif}} > t_\gamma$ in the system of a large size an approximately uniform solution (35) is developed. In the latter case to proceed consider the case $k \sim 1/R \ll k_m$, where R is the typical size of the system ($R = R_{f.o.}$ for the fireball formed in heavy-ion collisions). The spatially uniform solution of equation

$$\Delta_{\tilde{\epsilon}} \psi + 2\psi(1 - \psi^2) + \tilde{\epsilon} = \partial_\tau \psi$$

that follows from (8) in this case (as well as for seeds of a size $R_{\text{seed}} \ll R$ at $\beta \ll 1$, as we have argued above), is given by

$$\psi(t) = \pm 1 / \sqrt{1 + e^{-\tau} (1 - \psi_0^2) / \psi_0^2}, \quad (35)$$

where we for simplicity put $\tilde{\epsilon} \rightarrow 0$. Typical time needed for the initial amplitude $\psi_0 \ll 1$ to grow to $\psi(t \rightarrow \infty) \simeq \pm 1$ is $t_{\text{unif}} \sim t_0 \ln(1/\psi_0^2) \gg t_\gamma$.

Thus, we found some novel solutions describing evolution of fluctuations in the region of instability additionally to the uniform solution (35). For $k = \text{const} \neq 0$ we found periodic solutions given by (29), (31). For $k = k_0 \neq 0$ the solution yields minimum of the free energy for $t \rightarrow \infty$. For $k_0 = 0$, $\beta \gg 1$, we found quasiperiodic solutions (29), (31) with $k = k(t)$ from (34), yielding minimum of the free energy for $t \rightarrow \infty$.

6. Conclusions

According to our findings, signatures of QCD spinodal instabilities may be observed in experiments with heavy ions in some collision energy interval that corresponds to the first-order phase transition region of the QCD phase diagram. If typical time of the growth of a fluctuation in unstable region t_γ and of the fireball expansion $t_{f.o.}$ satisfy inequality $t_\gamma \lesssim t_{f.o.}$, one of the possible experimental signatures of the spinodal region would be manifestation of a spatially quasiperiodic structure with a typical period $r \simeq 2\pi/k_m$ in the rapidity spectra. If the parameter characterizing effective viscosity/inertia β were $\gg 1$, cf. Eq. (12), for $t_\gamma \ll t_{f.o.}$ one of the possible experimental signatures of the spinodal region would be manifestation of spatially quasiperiodic fluctuations with a typical size $r \sim 2\pi/k(t_{f.o.})$. However rough estimates done for the quark-hadron and nuclear gas-liquid first-order phase transitions in heavy-ion collisions [45–47] indicate that $\beta \ll 1$.

Concluding, we note that viscosity and thermal conductivity are driving forces of the first-order liquid-gas and quark-hadron phase transitions to the state with $k_0 = 0$, and the spinodal instability occurs for T below ITS line. The manifestation of a spatially quasiperiodic structures with a typical period $2\pi/k_m$, cf. Eq. (29), in the rapidity spectra in heavy-ion collisions in some collision energy interval could be interpreted as a signature of the occurrence of the spinodal instability at the first-order phase transition. For the second-order phase transition to the state with $k_0 \neq 0$, as for the case of the

pion condensation in dense nuclear matter, the periodic solution (29) holds for $k = k_0 \neq 0$, with k_0 not depending on time.

References

1. N. Aghanim et al. [Planck Collaboration], arXiv: 1807.06209.
2. A. D. Linde, "Phase Transitions in Gauge Theories and Cosmology," *Rept. Prog. Phys.* **1979**, 42, 389.
3. E. Witten, "Cosmic separation of phases," *Phys. Rev. D* **1984**, 30, 272.
4. J. Rafelski, "Connecting QGP-Heavy Ion Physics to the Early Universe," *Nucl. Phys. Proc. Suppl.* **2013**, 243, 155.
5. W. Busza, K. Rajagopal and W. van der Schee, "Heavy Ion Collisions: The Big Picture, and the Big Questions," *Ann. Rev. Nucl. Part. Sci.* **2018**, 68, 339.
6. B. V. Jacak and B. Muller, "The exploration of hot nuclear matter," *Science*. **2012**, 337, 310.
7. Z. Fodor, "Selected results in lattice quantum chromodynamics," *PTEP*. **2012**, 2012, 01A108.
8. S. Shapiro and S. A. Teukolsky, *Black Holes, White Dwarfs and Neutron Stars: The Physics of Compact Objects*, (Wiley, New York, 1983).
9. A.B. Migdal, E.E. Saperstein, M.A. Troitsky, and D.N. Voskresensky, *Phys. Rept.* **1990**, 192, 179.
10. H. J. Haubold, B. Kampfer, A. V. Senatorov and D. N. Voskresensky, "A Tentative approach to the second neutrino burst in SN1987A," *Astron. Astrophys.* **1988**, 191, L22.
11. P. Galeotti and G. Pizzella, "New analysis for the correlation between gravitational wave and neutrino detectors during SN1987A," *Eur. Phys. J. C* **2016**, 76, 426.
12. M. Prakash, I. Bombaci, M. Prakash, P. J. Ellis, J. M. Lattimer and R. Knorren, "Composition and structure of protoneutron stars," *Phys. Rept.* **1997**, 280 1.
13. B. P. Abbott *et al.* [LIGO Scientific and Virgo and 1M2H and Dark Energy Camera GW-E and DES and DLT40 and Las Cumbres Observatory and VINROUGE and MASTER Collaborations], "A gravitational-wave standard siren measurement of the Hubble constant," *Nature* **2017**, 551, 85.
14. P. Demorest, T. Pennucci, S. Ransom, M. Roberts and J. Hessels, "Shapiro delay measurement of a two solar mass neutron star," *Nature* **2010**, 467, 1081.
15. E. Fonseca, T. T. Pennucci, J. A. Ellis, I. H. Stairs, D. J. Nice, S. M. Ransom, P. B. Demorest, Z. Arzoumanian, K. Crowter, T. Dolch, R. D. Ferdman, M. E. Gonzalez, G. Jones, M. L. Jones, M. T. Lam, L. Levin, et al., "The NANOGrav nine-year data set: mass and geometric measurements of binary millisecond pulsars," *Astrophys. J.* **2016**, 832, 167.
16. J. Antoniadis, P. C. C. Freire, N. Wex, T. M. Tauris, R. S. Lynch, M. H. van Kerkwijk, M. Kramer and C. Bassa, "A massive pulsar in a compact relativistic binary," *Science* **2013**, 340 6131.
17. H.T. Cromartie, E. Fonseca, S. M. Ransom, P. B. Demorest, Z. Arzoumanian, H. Blumer, P. R. Brook, M. E. DeCesar, T. Dolch, J. A. Ellis, R. D. Ferdman, E. C. Ferrara, N. Garver-Daniels, P. A. Gentile, M. L. Jones, M. T. Lam, et al., "Relativistic Shapiro delay measurements of an extremely massive millisecond pulsar," *Nat. Astron.* **2019**, 4, 72.
18. E. V. Shuryak, "What RHIC experiments and theory tell us about properties of quark-gluon plasma?," *Nucl. Phys. A* **2005**, 750 64.
19. D. Teaney, J. Lauret and E. V. Shuryak, "A Hydrodynamic description of heavy ion collisions at the SPS and RHIC," arXiv: nucl-th/0110037.
20. P. Romatschke and U. Romatschke, "Viscosity Information from Relativistic Nuclear Collisions: How Perfect is the Fluid Observed at RHIC?," *Phys. Rev. Lett.* **2007**, 99, 172301.
21. E. Shuryak, "Physics of Strongly coupled Quark-Gluon Plasma," *Prog. Part. Nucl. Phys.* **2009**, 62 48.
22. G. Röpke, L. Münchow and H. Schulz, "Particle clustering and Mott transitions in nuclear matter at finite temperature," *Nucl. Phys. A* **1982**, 379, 536.
23. H. Schulz, D.N. Voskresensky, and J. Bondorf, "Dynamical aspects of the liquid-vapor phase transition in nuclear systems," *Phys. Lett. B* **1983**, 133, 141.
24. P. Chomaz, M. Colonna, and J. Randrup, "Nuclear spinodal fragmentation," *Phys. Rept.* **2004**, 389, 263.
25. J. Margueron and P. Chomaz, "A Unique spinodal region in asymmetric nuclear matter," *Phys. Rev. C* **2003**, 67, 041602.

26. K. A. Maslov and D. N. Voskresensky, "RMF models with σ -scaled hadron masses and couplings for the description of heavy-ion collisions below 2 A GeV," *Eur. Phys. J. A* **2019**, 55, 100.
27. D.G. Ravenhall, C.J. Pethick, and J.R. Wilson, "Structure Of Matter Below Nuclear Saturation Density," *Phys. Rev. Lett.* **1983**, 50, 2066.
28. T. Maruyama, T. Tatsumi, D.N. Voskresensky, T. Tanigawa, and S. Chiba, "Nuclear pasta structures and the charge screening effect," *Phys. Rev. C* **2005**, 72 015802.
29. A. B. Migdal, "Pion fields in nuclear matter," *Rev. Mod. Phys.* **1978**, 50, 107.
30. N. K. Glendenning, "Phase transitions and crystalline structures in neutron star cores," *Phys. Rept.* **2001**, 342 393.
31. T. Maruyama, T. Tatsumi, D. N. Voskresensky, T. Tanigawa, T. Endo and S. Chiba, "Finite size effects on kaonic pasta structures," *Phys. Rev. C* **2006**, 73, 035802.
32. D.N. Voskresensky, "On the possibility of the condensation of the charged rho meson field in dense isospin asymmetric baryon matter," *Phys. Lett. B* **1997**, 392, 262.
33. N. K. Glendenning, "First order phase transitions with more than one conserved charge: Consequences for neutron stars," *Phys. Rev. D* **1992**, 46, 1274.
34. H. Heiselberg, C. J. Pethick and E. F. Staubo, "Quark matter droplets in neutron stars," *Phys. Rev. Lett.* **1993**, 70, 1355.
35. D. N. Voskresensky, M. Yasuhira and T. Tatsumi, "Charge screening at first order phase transitions and hadron quark mixed phase," *Nucl. Phys. A* **2003**, 723, 291.
36. K. Maslov, N. Yasutake, A. Ayriyan, D. Blaschke, H. Grigorian, T. Maruyama, T. Tatsumi and D. N. Voskresensky, "Hybrid equation of state with pasta phases and third family of compact stars," *Phys. Rev. C* **2019**, 100, 025802.
37. A. Sedrakian and J. W. Clark, "Superfluidity in nuclear systems and neutron stars," *Eur. Phys. J. A* **2019**, 55, 167.
38. E. E. Kolomeitsev and D. N. Voskresensky, "Superfluid nucleon matter in and out of equilibrium and weak interactions," *Phys. Atom. Nucl.* **2011**, 74, 1316.
39. D. N. Voskresensky, "Vector-boson condensates, spin-triplet superfluidity of paired neutral and charged fermions, and $3P_2$ pairing of nucleons," arXiv:1911.07502 [nucl-th].
40. M. G. Alford, A. Schmitt, K. Rajagopal and T. Schäfer, "Color superconductivity in dense quark matter," *Rev. Mod. Phys.* **2008**, 80 1455.
41. D. N. Voskresensky, "The phase transition to an inhomogeneous condensate state," *Phys. Scripta* **29**, 259 (1984).
42. D. N. Voskresensky, "Quasiclassical description of condensed systems by a complex order parameter," *Phys. Scripta* **1993**, 47, 333.
43. E. E. Kolomeitsev and D. N. Voskresensky, "Negative kaons in dense baryonic matter," *Phys. Rev. C* **2003**, 68, 015803.
44. D.R. Tilley and J. Tilley, *Superfluidity and superconductivity*, Van Nostrand Reinhold Comp., N.Y., 1974.
45. V. V. Skokov and D. N. Voskresensky, "Hydrodynamical description of a hadron-quark first-order phase transition," *JETP Lett.* **90**, 223 (2009), arXiv: 0811.3868.
46. V. V. Skokov and D. N. Voskresensky, "Hydrodynamical description of first-order phase transitions: Analytical treatment and numerical modeling," *Nucl. Phys. A* **2009**, 828, 401.
47. V. V. Skokov and D. N. Voskresensky, "Thermal conductivity in dynamics of first-order phase transition," *Nucl. Phys. A* **2010**, 847, 253.
48. J. Steinheimer and J. Randrup, "Spinodal density enhancements in simulations of relativistic nuclear collisions," *Phys. Rev. C* **2013**, 87, 054903.
49. J. Steinheimer and J. Randrup, "Spinodal amplification and baryon number fluctuations in nuclear collisions at NICA," *Eur. Phys. J. A* **2016**, 52, 239.
50. D. N. Voskresensky, "Hydrodynamics of Resonances," *Nucl. Phys. A* **2011**, 849, 120.
51. L.I. Mandelstam and M.A. Leontovich, *Zh. Eksp. Teor. Fiz.* **1937**, 7, 438.
52. L.D. Landau and E.M. Lifshitz, *Fluid Mechanics*, Pergamon Press, Oxford, 1987.
53. E. E. Kolomeitsev and D. N. Voskresensky, "Viscosity of neutron star matter and r -modes in rotating pulsars," *Phys. Rev. C* **2015**, 91, 025805.

© 2020 by the authors. Submitted to *Universe* for possible open access publication under the terms and conditions of the Creative Commons Attribution (CC BY) license (<http://creativecommons.org/licenses/by/4.0/>).